Available online at www.sciencedirect.com
ScienceDirect
Carbohydrate Research 343 (2008) 101–112
Carbohydrate RESEARCH

Complete assignments of the ^{1}H and ^{13}C chemical shifts and $J_{H,H}$ coupling constants in NMR spectra of D-glucopyranose and all D-glucopyranosyl-D-glucopyranosides

Mattias U. Roslund,[a,*] Petri Tähtinen,[b] Matthias Niemitz[c] and Rainer Sjöholm[a,*]

[a]*Laboratory of Organic Chemistry, Åbo Akademi University, FI-20500 Åbo, Finland*
[b]*Department of Chemistry, University of Turku, FI-20014 Turku, Finland*
[c]*Department of Chemistry, University of Kuopio, FI-70211 Kuopio, Finland*

Received 13 August 2007; received in revised form 9 October 2007; accepted 11 October 2007
Available online 22 October 2007

Abstract—Complete assignment of the ^{1}H and ^{13}C NMR spectra of all possible D-glucopyranosyl-D-glucopyranosides was performed and the ^{1}H chemical shifts and proton–proton coupling constants were refined by computational spectral analyses (using PERCH NMR software) until full agreement between the calculated and experimental spectra was achieved. To support the experimental results, the ^{1}H and ^{13}C chemical shifts and the spin–spin coupling constants between the non-hydroxyl protons of α- and β-D-glucopyranose (**1a** and **1b**) were calculated with density functional theory (DFT) methods at the B3LYP/pcJ-2//B3LYP/6-31G(d,p) level of theory. The effects of different glycosidic linkage types and positions on the glucose ring conformations and on the α/β-ratio of the reducing end hydroxyl groups were investigated. Conformational analyses were also performed for anomerically pure forms of methyl D-glucopyranosides (**13a** and **13b**) and fully protected derivatives such as 1,2,3,4,6-penta-*O*-acetyl-D-glucopyranoses (**14a** and **14b**).

Keywords: Glucose; D-Glucosyl-D-glucosides; NMR spectroscopy; DFT; Proton chemical shifts; Carbon chemical shifts; Computational spectral analysis; Homonuclear spin–spin coupling constants; Conformation

1. Introduction

The structural analysis of carbohydrates is not a simple task and usually it is necessary to utilize several analytical methods in a complementary way. For example, X-ray crystallographic studies require suitable crystals for diffraction measurements, and it is generally difficult to obtain sufficiently good crystals from carbohydrates. NMR spectroscopy provides a powerful arsenal of tools for analyzing the primary structures of carbohydrates, and it is the only experimental method by which it is possible to analyze the conformations and dynamics of sugars in their natural environment: water. Because of their versatility, NMR spectroscopic methods have been widely utilized in the structural studies of carbohydrates.[1] However, for the analyses of oligosaccharide structures the measurements and interpretation of the results can be very demanding and time consuming.[2]

The complete ^{1}H and ^{13}C NMR signal assignments for all 19 α- and β-D-glucosyl-D-glucosides (Scheme 1, **2**–**12**) have not been reported earlier. Moreover, most of the published data available are contradictory.[3–12] Part of the published data is from selectively protected sugars, for example, sugars methylated at the anomeric center to hinder mutarotation and so enabling assignment of the α- and β-anomerically pure saccharides separately with less overlapping signals. The ^{13}C chemical shifts of some anomerically locked glucosyl glucosides have been determined using dynamic NMR, and they have also been compared with those of the monomer

* Corresponding authors. Tel.: +358 2 2154501; fax: +358 2 2154866 (M.U.R.); tel.: +358 2 2154134; fax: +358 2 2154866 (R.S.); e-mail addresses: mattias_roslund@yahoo.com; rsjoholm@abo.fi

0008-6215/$ - see front matter © 2007 Elsevier Ltd. All rights reserved.
doi:10.1016/j.carres.2007.10.008

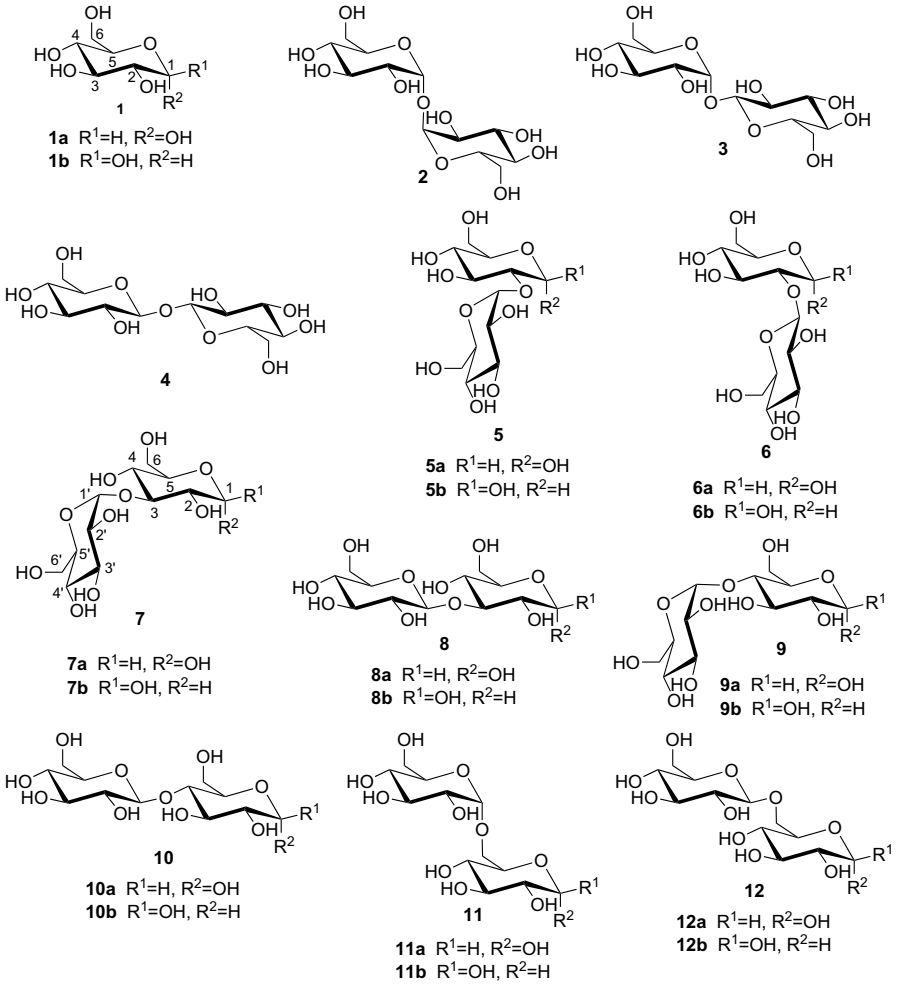

Scheme 1. Glucopyranose is shown with all differently linked [(1↔1) (trehaloses), (1→2) (kojibiose and sophorose), (1→3) (nigerose and laminaribiose), (1→4) (maltose and cellobiose), and (1→6) (isomaltose and gentiobiose)] glucose-based disaccharides investigated in this study.

D-glucose.[10–12] Also, some proton chemical shifts for glucose-based disaccharides have been determined earlier,[10,12,13] and information about the coupling constants was supplied by De Bruyn et al.[13] in 1975.

The results of an earlier investigation aided by ^{13}C labeling of the concentrated solutions of aldohexoses in water showed that almost all forms of D-glucose (**1**) are present in solution (Fig. 1): α-pyranose 38% (**1a**), β-pyranose 62% (**1b**), β-furanose 0.14% (**1d**), and the aldehyde form 0.002% (**1e**).[14] In a more recent investigation of aldohexoses in water it was shown by using ^{13}C labeling at the C1 terminus that all five- and six-membered ring forms of D-glucose are present at equilibrium at 30 °C [α-pyranose 37.63%, β-pyranose 61.96%, α-furanose 0.108% (**1c**), β-furanose 0.28%, aldehyde 0.0040%, and hydrate form 0.0059% (**1f**)].[15] Seven-membered ring forms were not detected.[15]

The conformational space of α- and β-D-glucose has been widely studied with experimental and theoretical methods, but there are still many questions to be answered.[16] In most studies it has been found that the

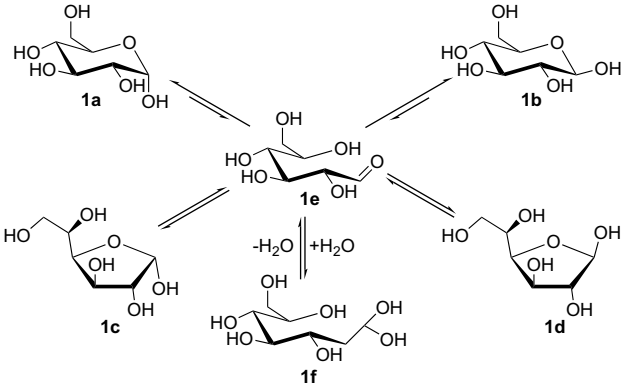

Figure 1. Different forms of D-glucose in solution determined by ^{13}C NMR spectroscopy.[15]

$^4C_1$ chair is the dominant ring conformation in aqueous solution for both anomers.[17–19] In vacuo the α-anomer is more stable than the β-anomer because of the anomeric effect, but in aqueous solution the α/β ratio is reversed due to solvent effects and hydrogen bonding.[20] For both

the α- and the β-anomers, three rotamers due to the hydroxymethyl side chain orientation are populated.[19,21–28] These rotamers are defined by the O5–C5–C6–O6 torsion angle, which is about −60° in the *gg*, 60° in the *gt*, and 180° in the *tg* conformation. Furthermore, the results of the theoretical studies have shown that the conformations, which involve cooperative anticlockwise orientation of intramolecularly hydrogen-bonded hydroxyl groups, represent the most stable ones in gas-phase.[29] On the contrary, some experimental and theoretical results have been reported indicating that the cooperative orientation of the hydroxyl groups is perturbed in aqueous solution due to intermolecular hydrogen bonding to the solvent molecules.[20,22,30–32] However, other theoretical studies have shown that the hydroxyl groups can still remain anticlockwise oriented even though hydrogen bonds are formed between the glucose hydroxyl groups and the solvent molecules.[33–35]

Previously, the conformation around the glycosidic linkage of some glucose based disaccharides had been investigated by theoretical calculations.[36–38] Also, the ring conformations, as well as, the position of the hydroxyl groups have been investigated by several groups.[17,39–43] Furthermore, the orientation of the hydroxymethyl group has been investigated using NMR spectroscopic methods[44] and theoretical calculations in solution, as well as, in gas-phase.[45,46] The influence of the hydrogen bonding of the hydroxyl groups on the disaccharide conformations has been investigated by replacing all hydroxyl groups with fluorine atoms, as fluorine has approximately the same size as a hydroxyl group but it does not permit hydrogen bonding.[47] Furthermore, the secondary structure of some mono-, oligo-, and polysaccharides has been investigated by vibrational Raman optical activity (VROA) spectroscopy.[48,49] Recently, a vibrational circular dichroism (VCD) study of discrimination of the glycosidic linkage position and stereochemistry (α or β) of glucodisaccharides was published.[50] Both, reducing and non-reducing glucobioses showed different VCD spectral features in comparison to their constituent D-glucose and the anomerically locked model compounds investigated. Inter- and intramolecular hydrogen bonding was suggested to cause these spectral differences.[50]

In this work, the complete assignments of ^{1}H, as well as, ^{13}C NMR spectra for compounds **1**–**14** (Schemes 1 and 2) are presented. The spectral assignments were based on 1D proton and carbon NMR experiments in combination with proton 1D TOCSY spectroscopy and a set of 2D NMR experiments (*J*-resolved spectroscopy, DQF-COSY, TOCSY, HSQC, HMBC, HSQC–TOCSY, and INADEQUATE) recorded with sufficient resolution to separate ^{1}H and ^{13}C correlations and chemical shifts from the 2D matrix. The chemical shifts and coupling constants were then refined and the different populations were optimized by iterative spectral analysis using PERCH NMR software.[51]

13a R^1=H, R^2=OCH_3
13b R^1=OCH_3, R^2=H

14a R^1=H, R^2=OAc
14b R^1=OAc, R^2=H

Scheme 2.

Only the pyranose forms of the sugars were investigated in this work, because all the other forms are present in very low concentrations in aqueous solution. Furthermore, no furanose- or open forms were detected in the dilute samples prepared for ^{1}H NMR spectra analyses, so there was no need to include them in the spectral analyses. In the high-concentration samples for INADEQUATE measurements some extra sugar signals were observed (<0.2%). The α/β ratio was determined from the proton spectrum by the integration of the anomeric proton signals. The influence of the glycosidic linkage position on the anomerization equilibrium was investigated for the studied samples at 30 °C in water. Additionally, the conformations of the anomeric forms of the methyl glycopyranosides (**13a** and **13b**) were investigated in D_2O and the peracetylated α- and β-D-glucopyranoses (**14a** and **14b**) in $CDCl_3$ at 30 °C (Scheme 2).

Furthermore, to support the experimental results, the ^{1}H and ^{13}C chemical shifts and the spin–spin coupling constants between the non-hydroxyl protons for several forms of α- and β-D-glucose were calculated using density functional theory (DFT) methods.

2. Results and discussion

The structures of D-glucopyranose (**1**) and all of the investigated 19 disaccharides, α,α-trehalose (**2**), α,β-trehalose (**3**), β,β-trehalose (**4**), kojibiose (**5**), sophorose (**6**), nigerose (**7**), laminaribiose (**8**), maltose (**9**), cellobiose (**10**), isomaltose (**11**), and gentiobiose (**12**) are presented in Scheme 1 where also the numbering of the atoms is shown for compounds **1** and **7**.

Generally, with the exception of the anomeric protons of the disaccharides, the proton resonances of these compounds display a rather narrow range of chemical shifts, which makes detailed spectral analyses very difficult, even at the high magnetic fields available today. A useful strategy for the structure determination of carbohydrates is the complementary use of 1D and 2D ^{1}H and ^{13}C NMR spectroscopy. In principle, the resonance assignment of at least one of the two spectra should be achieved independently and could so serve as a starting point for the construction of the two-dimensional (2D)

heteronuclear chemical shift correlations. However, the signals of certain types of protons and carbons (e.g., H1, C1, and C6) are more easily assigned than others, and therefore these easily identified ^{1}H and ^{13}C signals can be used in a complementary fashion.

2.1. Carbon-13 NMR spectra

In the carbon spectra of gluco-oligosaccharides (Scheme 1) three chemical shift regions for the signals are usually seen resulting from the anomeric (90–105 ppm), methine (69–83 ppm), and methylene carbons (61–69 ppm). The ^{13}C chemical shifts for the studied compounds are collected in Table 1.

2.2. Proton NMR spectra

The signals of the anomeric protons are usually easily identified because they are well-resolved in the low-field region of the spectrum between 4.5 and 5.4 ppm and each signal appears as a doublet (d) or as a broadened doublet due to additional long-range couplings to H3 and H5 (Tables 2 and S1, Supplementary data). All the other non-hydroxylic protons appear as doublets of doublets (dd), except H5 that has couplings to H4, H6a, and H6b (ddd) (Table 2).

Interestingly, in many cases long-range proton–proton couplings were observed for the α-anomers (see Table S1) and were also reproduced by the DFT calculations. All the non-anomeric proton signals of the glucose moiety appeared within 0.7 ppm in the region 3.2–3.9 ppm, resulting in higher order NMR spectra typically observed for carbohydrates (Table 2). The signals of the anomeric protons in the non-reducing unit of the α- or β-disaccharides were close to each other whereas those of the reducing unit at α- and β-equilibrium were well separated. The α- and β-forms were easily identified from their $^{3}J_{H1,H2}$ and $^{1}J_{C1,H1}$ values. For example, for the α-D-glucopyranose the $^{3}J_{H1,H2}$ is 3.8 Hz and $^{1}J_{C1,H1}$ is 169.8 Hz, while for the β-anomer the couplings are 8.0 and 161.3 Hz, respectively (cf. Table 2). Similar values had also been observed in earlier studies.[52] The magnitudes of the $^{1}J_{C1,H1}$ are reversed for the corresponding L-isomers.[53]

The experimental ^{1}H chemical shifts are collected in Table 2 with their vicinal and geminal coupling constants measured at 500 MHz. The long-range couplings are left out from Table 2 for clarity but are presented in the Supplementary data (Table S1).

Table 1. ^{13}C NMR chemical shifts of all the studied mono- and disaccharides (see Schemes 1 and 2) in D_2O at 30 °C (**14a** and **14b** were measured in $CDCl_3$ and referenced to TMS δ_C 0.00 ppm)

	C1	C2	C3	C4	C5	C6	C1′	C2′	C3′	C4′	C5′	C6′
1a	92.77	72.15	73.43	70.32	72.10	61.27						
1b	96.59	74.81	76.43	70.27	76.61	61.42						
13a[a]	99.92	71.87	73.74	70.22	72.23	61.21						
13b[b]	103.88	73.75	76.42	70.31	76.57	61.41						
14a	89.12	69.26	69.90	67.98	69.88	61.53						
14b	91.77	70.32	72.85	67.86	72.79	61.52						
2							93.93	71.71	73.20	70.37	72.83	61.20
3[c]							100.92	72.12	73.50	70.09	73.37	61.12
3[d]							103.64	73.81	76.09	70.09	76.85	61.31
4							99.85	73.32	76.41	70.18	76.75	61.32
5a	90.12	76.59	71.88	70.25	71.97	61.24	97.00	72.07	73.45	70.08	72.50	61.00
5b	96.93	79.24	75.12	70.42	76.42	61.45	98.40	72.12	73.46	70.01	72.34	60.93
6a	92.42	81.39	72.36	70.10	71.77	61.19	104.55	73.93	76.22	70.10	76.40	61.26
6b	95.25	82.07	76.48	70.08	71.47	61.31	103.33	74.17	76.24	70.26	76.70	61.47
7a	92.93	70.78	80.36	70.69	71.87	61.06	99.77	72.37	73.56	70.11	72.44	61.05
7b	96.66	73.52	82.87	70.72	76.32	61.24	99.72	72.31	73.57	69.99	72.42	60.90
8a	92.70	71.67	83.13	68.81	71.90	61.23	103.61	74.17	76.25	70.26	76.67	61.40
8b	96.38	74.46	85.39	68.84	76.24	61.36	103.53	74.14	76.26	70.26	76.70	61.37
9a	92.58	71.97	73.90	77.63	70.64	61.27	100.34	72.44	73.55	70.03	73.34	61.16
9b	96.46	74.69	76.88	77.43	75.25	61.42	100.25	72.34	73.53	70.01	73.36	61.16
10a	92.46	71.87	71.98	79.43	70.75	60.60	103.20	73.82	76.16	70.12	76.63	61.25
10b	96.39	74.54	74.94	79.30	75.43	60.73	103.16	73.81	76.16	70.11	76.63	61.23
11a	92.85	72.07	73.67	70.20	70.69	66.42	98.63	72.16	73.72	70.15	72.46	61.11
11b	96.73	74.70	76.61	70.05	74.95	66.34	98.59	72.12	73.73	70.15	72.42	61.11
12a	92.77	72.05	73.30	70.06	71.07	69.28	103.30	73.72	76.29	70.24	76.52	61.37
12b	96.61	74.66	76.27	70.11	75.52	69.44	103.33	73.72	76.27	70.25	76.56	61.36

[a] ^{13}C chemical shift for $-OCH_3$ is 55.66 ppm.
[b] ^{13}C chemical shift for $-OCH_3$ is 57.82 ppm.
[c] α-Anomer part.
[d] β-Anomer part of the non-reducing α,β-trehalose disaccharide.

Table 2. Proton chemical shifts reported in ppm and $J_{H,H}$ coupling constants (Hz, in parentheses) of the studied compounds

	H1	H2	H3	H4	H5	H6a	H6b	H1′	H2′	H3′	H4′	H5′	H6a′	H6b′
	$^3J_{H1,H2}$	$^3J_{H2,H3}$	$^3J_{H3,H4}$	$^3J_{H4,H5}$	$^3J_{H5,H6a/H6b}$	$^2J_{H6a,H6b}$		$^3J_{H1',H2'}$	$^3J_{H2',H3'}$	$^3J_{H3',H4'}$	$^3J_{H4',H5'}$	$^3J_{H5',H6a'/\ H6b'}$	$^2J_{H6a',H6b'}$	
1a	5.214	3.516	3.696	3.393	3.817	3.823	3.745							
	(3.80)	(9.84)	(9.17)	(9.99)	(2.31, 5.40)	(−12.37)								
1b	4.627	3.226	3.469	3.385	3.447	3.879	3.704							
	(7.97)	(9.46)	(9.17)	(9.92)	(2.27, 5.95)	(−12.30)								
13a[a]	4.796	3.547	3.653	3.388	3.632	3.856	3.744							
	(3.83)	(9.81)	(9.14)	(10.10)	(2.32, 5.58)	(−12.30)								
13b[a]	4.364	3.247	3.474	3.366	3.447	3.912	3.710							
	(8.00)	(9.45)	(9.16)	(9.92)	(2.31, 6.14)	(−12.34)								
14a	6.334	5.101	5.472	5.141	4.119	4.099	4.267							
	(3.71)	(10.29)	(9.49)	(10.35)	(2.32, 4.14)	(−12.51)								
14b	5.718	5.137	5.250	5.129	3.837	4.117	4.288							
	(8.33)	(9.58)	(9.39)	(10.11)	(2.25, 4.57)	(−12.50)								
2								5.178	3.633	3.835	3.434	3.809	3.843	3.746
								(3.86)	(9.94)	(9.12)	(10.09)	(2.33, 5.43)	(−12.35)	
3[b]								5.222	3.583	3.734	3.434	3.923	3.823	3.744
								(3.78)	(9.92)	(9.16)	(10.26)	(2.28, 5.22)	(−12.31)	
3[c]								4.634	3.400	3.513	3.395	3.468	3.861	3.705
								(7.98)	(9.54)	(9.15)	(9.97)	(2.30, 5.75)	(−12.39)	
4								4.805	3.346	3.502	3.406	3.463	3.902	3.721
								(8.07)	(9.47)	(9.15)	(9.93)	(2.31, 6.05)	(−12.38)	
5a	5.426	3.623	3.803	3.447	3.847	3.832	3.780	5.083	3.543	3.776	3.444	3.931	3.828	3.757
	(3.55)	(9.77)	(9.07)	(10.18)	(2.35, 4.43)	(−12.30)		(3.80)	(9.95)	(8.95)	(10.06)	(2.34, 5.30)	(−12.51)	
5b	4.784	3.372	3.560	3.409	3.448	3.883	3.704	5.373	3.533	3.737	3.450	4.019	3.809	3.772
	(7.95)	(9.40)	(9.13)	(9.93)	(2.22, 5.90)	(−12.31)		(3.89)	(9.94)	(9.18)	(10.18)	(2.54, 4.64)	(−12.61)	
6a	5.428	3.628	3.848	3.447	3.826	3.824	3.750	4.615	3.353	3.490	3.405	3.438	3.888	3.722
	(3.68)	(9.78)	(9.21)	(10.08)	(2.39, 5.27)	(−12.29)		(7.92)	(9.46)	(9.18)	(9.92)	(2.26, 5.62)	(−12.41)	
6b	4.707	3.506	3.680	3.421	3.455	3.878	3.710	4.772	3.321	3.501	3.374	3.442	3.911	3.702
	(7.91)	(9.30)	(9.39)	(9.92)	(2.17, 5.75)	(−12.35)		(7.98)	(9.49)	(9.11)	(9.89)	(2.22, 6.33)	(−12.40)	
7a	5.219	3.611	3.838	3.630	3.840	3.814	3.750	5.358	3.556	3.740	3.432	3.998	3.828	3.763
	(3.82)	(9.73)	(8.95)	(10.33)	(2.33, 5.23)	(−12.33)		(3.91)	(9.91)	(9.16)	(10.17)	(2.39, 4.78)	(−12.34)	
7b	4.650	3.319	3.627	3.625	3.459	3.872	3.705	5.343	3.549	3.736	3.449	4.001	3.800	3.781
	(8.03)	(9.35)	(8.72)	(9.85)	(2.27, 5.85)	(−12.32)		(3.91)	(9.92)	(9.15)	(10.19)	(2.31, 4.35)	(−12.30)	
8a	5.221	3.709	3.895	3.504	3.852	3.821	3.769	4.702	3.350	3.515	3.400	3.482	3.908	3.711
	(3.79)	(9.70)	(8.96)	(9.91)	(2.26, 4.92)	(−12.26)		(7.98)	(9.50)	(9.16)	(9.91)	(2.26, 6.27)	(−12.28)	
8b	4.660	3.421	3.722	3.500	3.476	3.884	3.723	4.720	3.348	3.509	3.396	3.471	3.905	3.706
	(8.05)	(9.31)	(8.96)	(10.04)	(2.07, 5.56)	(−12.33)		(7.96)	(9.50)	(9.14)	(9.95)	(2.29, 6.22)	(−12.33)	
9a	5.215	3.555	3.955	3.631	3.925	3.836	3.797	5.391	3.568	3.684	3.405	3.719	3.843	3.753
	(3.81)	(9.92)	(8.97)	(10.05)	(2.22, 4.81)	(−12.17)		(3.91)	(9.92)	(9.18)	(10.07)	(2.30, 5.28)	(−12.40)	
9b	4.638	3.261	3.753	3.628	3.581	3.897	3.753	5.392	3.568	3.669	3.406	3.704	3.841	3.751
	(7.98)	(9.56)	(8.86)	(9.84)	(2.11, 5.37)	(−12.22)		(3.93)	(9.94)	(9.20)	(10.06)	(2.25, 5.27)	(−12.39)	
10a	5.212	3.566	3.812	3.629	3.937	3.873	3.846	4.501	3.312	3.498	3.411	3.478	3.907	3.726
	(3.79)	(9.85)	(9.12)	(9.66)	(2.24, 4.61)	(−12.38)		(7.96)	(9.50)	(9.18)	(9.90)	(2.25, 5.89)	(−12.43)	
10b	4.649	3.273	3.615	3.639	3.586	3.942	3.797	4.499	3.304	3.496	3.409	3.476	3.905	3.725
	(7.99)	(9.37)	(9.07)	(9.83)	(2.19, 5.14)	(−12.28)		(7.95)	(9.49)	(9.16)	(9.93)	(2.27, 5.92)	(−12.37)	

(*continued on next page*)

Table 2 (*continued*)

	H1	H2	H3	H4	H5	H6a	H6b	H1′	H2′	H3′	H4′	H5′	H6a′	H6b′
	$^3J_{H1,H2}$	$^3J_{H2,H3}$	$^3J_{H3,H4}$	$^3J_{H4,H5}$	$^3J_{H5,H6a/H6b}$	$^2J_{H6a,H6b}$		$^3J_{H1',H2'}$	$^3J_{H2',H3'}$	$^3J_{H3',H4'}$	$^3J_{H4',H5'}$	$^3J_{H5',H6a'/H6b'}$	$^2J_{H6a',H6b'}$	
11a	5.228	3.530	3.694	3.503	3.997	3.691	3.983	4.937	3.541	3.720	3.415	3.699	3.835	3.755
	(3.81)	(9.85)	(9.16)	(10.09)	(2.22, 4.39)	(−11.27)		(3.72)	(9.89)	(9.15)	(9.85)	(2.18, 5.27)	(−12.43)	
11b	4.659	3.242	3.470	3.505	3.626	3.748	3.941	4.943	3.544	3.725	3.415	3.721	3.838	3.752
	(7.98)	(9.43)	(9.18)	(9.86)	(2.04, 4.73)	(−11.24)		(3.73)	(9.85)	(9.08)	(10.23)	(2.23, 5.25)	(−12.27)	
12a	5.213	3.525	3.701	3.489	3.971	4.135	3.874	4.482	3.300	3.483	3.380	3.445	3.904	3.712
	(3.79)	(9.83)	(9.23)	(10.18)	(2.11, 5.07)	(−11.44)		(8.00)	(9.47)	(9.18)	(9.92)	(2.26, 6.10)	(−12.30)	
12b	4.640	3.241	3.475	3.453	3.615	4.190	3.833	4.499	3.306	3.486	3.380	3.452	3.907	3.713
	(7.99)	(9.41)	(9.19)	(9.79)	(2.05, 6.02)	(−11.48)		(7.99)	(9.47)	(9.14)	(9.92)	(2.29, 6.05)	(−12.37)	

[a] Proton chemical shift for the $-OCH_3$ group in **13a** at 3.407 ppm and **13b** at 3.559 ppm.
[b] α-Anomer part.
[c] β-Anomer part of the non-reducing α,β-trehalose disaccharide.

To display the general appearance of the proton NMR spectra of the glucopyranosyl glucopyranosides the ^{1}H NMR spectrum of the anomeric mixture of one of the studied disaccharides, laminaribiose (β-D-Glc*p*-(1→3)-D-Glc*p*) is shown in Figure 2 together with the calculated spectrum from PERCH NMR software.

2.3. Anomeric ratios

The populations of different anomers at equilibrium in aqueous solution at 30 °C are shown in Table 3. The results clearly indicate that the anomeric ratio for the reducing unit in these commercially available glucobioses is significantly affected when the non-reducing unit is coupled with a (1→2) linkage (**5** and **6**). This is probably due to the cooperation of steric hindrance and intramolecular hydrogen bonding. From the optimized structures, used for the prediction of NMR parameters (PERCH NMR software), the following hydrogen bond possibilities were observed: for the β-(1→2)-linked α-sophorose (**6a**) hydrogen bonds from 1-OH to O2 in the glycosidic linkage and from 3-OH to 2′-OH are likely. The hydrogen bonds found for the β-sophorose (**6b**) are slightly longer due to its geometry. For the α-anomer of the α-(1→2)-linked α-kojibiose (**5a**) hydrogen bonds are favorable from 1-OH to O2 and from 3-OH to 6′-OH while the β-kojibiose (**5b**) shows hydrogen bonds from 3-OH to the oxygen in the glycosidic linkage and from 1-OH to 2′-OH. For the more linearly linked β-(1→3) disaccharide **8**, the α-anomer is slightly more favorable, which has been proposed also by VROA studies.[49] The other disaccharides studied were similar to the D-glucose dissolved in water possessing a 62:38 of β/α ratio.

2.4. PERCH NMR software

The ^{1}H chemical shifts and coupling constants for all the 25 investigated compounds were refined by iterative spectral analysis using both the integral transform mode, as well as the total-line-shape fitting mode of PERCH's iterator PERCHit.[54] Starting values for the iterative spectral analyses were extracted from the experimental spectra directly. The large variety of 1D and 2D-data allowed very reasonable starting values for chemical shifts and *J*-couplings, so the iteration usually converged straightforwardly when starting with a rather small line-broadening of 10–20 Hz in the integral transform mode. In case of ambiguous assignments, the different possibilities were iterated separately until no further improvement was achievable. The spectral parameters were finally adjusted using the total-line-shape fitting mode including optimization of individual line-widths and the line-shape (Gaussian/Lorentzian contribution). In all cases, the overall RMS for the difference between experimental and calculated

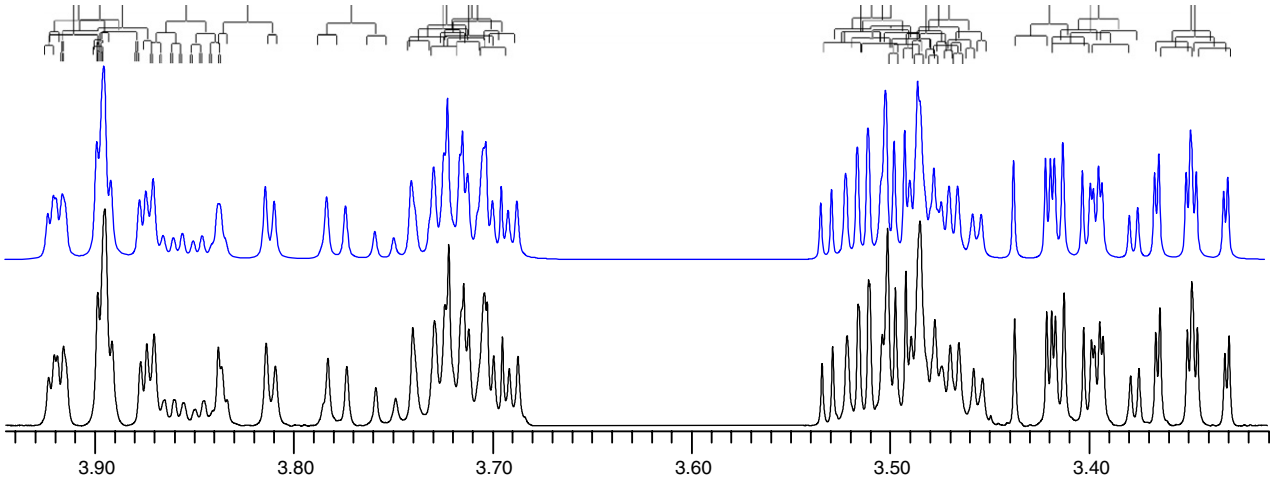

Figure 2. The crowded non-anomeric region of the experimental (lower) and calculated (upper) proton NMR spectrum of laminaribiose (**8**) (24 protons).

Table 3. The anomeric ratios of the studied compounds presented as percentages of the axial and equatorial hydroxyl groups at the reducing unit based on the integration of the anomeric ^{1}H NMR signals

Compound	**1**	**5**	**6**	**7**	**8**	**9**	**10**	**11**	**12**
α-Anomer (%)	37.5	48.1	73.3	38.4	44.1	38.9	38.1	38.4	38.3
β-Anomer (%)	62.5	51.9	26.7	61.6	55.9	61.1	61.9	61.6	61.7

spectra was below 0.1%. Due to the fact that the line-widths and line-shapes were part of the final refinement of the spectral parameters, the accuracy of the parameters can be in the order of the digital resolution (0.09 Hz) or even better.[54] The standard deviations for the ^{1}H chemical shifts were found to be well below 0.1 Hz and therefore could be given with four digits. The standard deviations for the *J*-couplings were in the same range or better and therefore given with at least three digits. This iterative fitting provides the most accurate spectral parameters, and complete agreement of the extracted spectral parameters with the experimental spectrum should always be tested by calculating the spectrum and comparing it to the experimental one (Fig. 2), especially when the parameters have been extracted using 2D-methods and the spectrum features higher order effects as in most of these cases.

2.5. NMR results and discussion

The observed two spin systems (α- and β-spin system) for glucose and the four spin systems for the disaccharides are due to the anomeric α- and β-configurations of the reducing unit, giving different ^{1}H and ^{13}C chemical shifts and coupling constants for both the reducing and the non-reducing part of the disaccharide. The three non-reducing trehaloses are of course an exception to this, because the anomeric configuration is locked, and therefore no mutarotation occurs.

Steric hindrance, hydrogen bonding, and electronic effects (proximity effects) could cause the chemical shift differences in the investigated sugars. As can be seen in Table 1, with the high field spectrometers available today, in most cases the differences in the carbon chemical shifts at the non-reducing end can be observed for the α- and β-forms of the reducing end.

Only very small differences between the experimental and the iterated spectra were observed. Some of these differences arise from impurities in the commercial products but also due to additional very small ^{1}H–^{1}H long-range couplings. These small discrepancies can partially be solved by the versatility of the PERCH program, which allows the determination of different line-widths for different spin particles and therefore long-range couplings smaller than the line-widths were usually neglected. The ^{1}H and ^{13}C chemical shifts and coupling constants for all the investigated compounds were also predicted using PERCH MMS software[55] and found to be in very good agreement with the experimentally determined parameters.

The assignment for the three non-reducing disaccharides (trehaloses **2**–**4**) can be based on the assignment of the α- and β-anomers of glucose, except for the anomeric carbon. With the exception of the three trehaloses (**2**–**4**), it was observed that the reducing anomeric α-carbon usually resonates in the region 90.1–92.9 ppm while the β-carbon resonates at 95.3–96.9 ppm (Table 1). The α-linked anomeric carbon of the non-reducing end resonates in the region 97.0–104.6 ppm, while the β-linked non-reducing anomeric carbon resonates at 98.4–103.5 ppm (Table 1). The results also show that the chemical shift of the anomeric carbon in the reducing

end of the β-anomer is shifted several ppm downfield (≈96 ppm) from that of the α-anomer (≈93 ppm). Also the non-reducing anomeric carbon signal of the disaccharides with an α-glycosidic linkage resonates at a higher field than the β-linked disaccharide (Table 1).

The position of the linkage in disaccharides may also be determined by observing which ^{13}C resonances of the residue undergo a 4–10 ppm downfield shift upon O-glycosidation. This is seen, for example, in the C6 chemical shifts of the 1→6 linked disaccharides **11** (66.4 ppm) and in **12** (69.4 ppm) when compared to the corresponding chemical shifts at approximately 61.3 ppm for all the other unprotected sugars. As it can be observed from Table 1 the β-configuration induced a 4 ppm downfield shift of C1 and C1′. The reducing end C1 resonates around 96.5 ppm for the β-sugar and at 92.5 ppm for the α-mono- or disaccharide. The same tendency is observed for the non-reducing unit anomeric carbon chemical shifts (103 ppm for the β-linkage and 99 ppm for α-linked disaccharides) (Table 1).

It is very challenging to analyze both the ^{13}C and the ^{1}H NMR spectra, and the information found in the literature with variable assignments achieved by the use of different NMR techniques, sample concentrations, solvents, and temperatures, does not provide much help.[3–13] In many cases the poor resolution of a spectrum can become a problem. That is why NMR spectroscopic analyses of larger glucose oligosaccharides than glucobioses can be very complicated, especially if the moieties are identical and are connected by the same types of linkages. The proton and carbon NMR spectra of maltose and maltotriose are almost identical, and mainly in the carbon spectra more signals are observed for the glucotriose than for the glucobiose. Therefore, when working with larger molecules, it is better to utilize the carbon spectrum and then move from the 2D hetero correlation spectra (HSQC, HMBC, and HSQC–TOCSY) to the proton spectra (coupling constants can be helpful in assigning different sugar monomers) and to the different homonuclear 2D correlation spectra (COSY and TOCSY). 2D *J*-resolved spectroscopy can be very useful for the elucidation of complicated and strongly overlapping proton multiplets. The chemical shift and the ^{1}H–^{1}H couplings are separated into two different dimensions (the magnitude of the coupling from the *F*1 axis and the chemical shift in the direct dimension). In the 2D INADEQUATE spectrum direct ^{13}C–^{13}C connections are shown. The sensitivity for this 'COSY' type experiment is very low because the natural abundance of ^{13}C is just over one percent, and the probability of finding one ^{13}C attached to another ^{13}C isotope is only one in 10,000. Therefore, the use of INADEQUATE is mainly limited to very concentrated solutions or ^{13}C-labeled samples.

2.6. Theoretical calculations

To support the experimental results, the ^{13}C and the non-hydroxyl ^{1}H chemical shifts and the spin–spin coupling constants between the non-hydroxyl protons of α- and β-D-glucose were calculated with DFT methods. Theoretical computation of NMR parameters by DFT methods is nowadays at a level where useful accuracy for structural chemistry studies is achieved at a reasonable computational cost.[56,57] On the basis of the reasoning by da Silva et al., a set of three conformers for α-D-glucose and five for β-D-glucose depicted in Figure 3 were chosen to represent their average structures, although the existence of other types of conformations in aqueous solution cannot be excluded, but it is assumed that such conformers are less stable than the chosen ones.[21] The relative stability differences of the conformers in solution were obtained by calculating their free energy differences (ΔG°) at the B3LYP/6-31G(d,p) level and adding to them the corresponding solvation energies calculated for each conformer at the B3LYP/6-311G++(2d,2p) level. These relative stability differences of the conformers in solution were then used

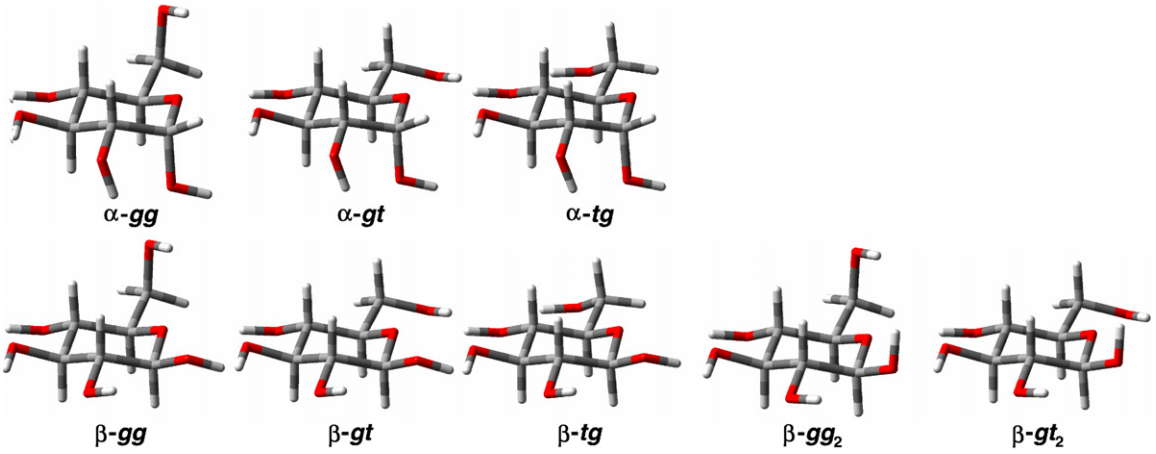

Figure 3. The conformers of α- and β-D-glucopyranose used for the DFT calculations of spin–spin coupling constants.

to estimate the conformer populations by assuming Boltzmann distribution between the conformers (see Tables S2–S7, Supplementary data).[21]

For the optimized structures, the ^{1}H and ^{13}C nuclear shielding constants and all the contributing terms to the nuclear spin–spin coupling constants were calculated at the B3LYP/pcJ-2 level. The correlation between the population weighted averages (pwa) of the calculated ^{1}H chemical shifts and the corresponding experimental values (cf. Table 4) is surprisingly good [$R_{(average)} = 0.977$] considering that solvent effects were not included in the geometry optimizations and NMR parameter calculations. The largest absolute deviations between the calculated and experimental values are less than 0.25 ppm (7%) and the overall mean absolute deviation (MAD) is only 0.1 ppm (2.6%). Also, the calculated ^{13}C chemical shifts correlate very well with the experimental values [cf. Table 5; $R_{(average)} = 0.9996$]. However, the calculated chemical shifts are systemically about 10 ppm (13.4%) larger in average than the corresponding experimental values. The correlation between the population weighted averages of the calculated couplings and the experimental results (cf. Table 6) is good [$R_{(average)} = 0.995$], although, in some cases the deviations are quite large. For example, the calculated $^{3}J_{H1,H2}$ for the α-anomer deviates about 0.8 Hz (21%)

Table 4. Comparison of the calculated and the experimental (D_2O, 30 °C) δ_H values (ppm) of α-(**1a**) and β-D-glucopyranose (**1b**)

	α-D-Glucopyranose (**1a**)				β-D-Glucopyranose (**1b**)			
	Calcd	Exptl.	Δδ (ppm)	|Δδ| (%)	Calcd	Exptl.	Δδ (ppm)	|Δδ| (%)
H1	5.301	5.214	0.087	1.67	4.586	4.627	−0.040	0.87
H2	3.273	3.516	−0.244	6.93	3.152	3.226	−0.074	2.29
H3	3.653	3.696	−0.043	1.15	3.478	3.469	0.009	0.25
H4	3.589	3.393	0.196	5.77	3.614	3.385	0.229	6.76
H5	3.907	3.817	0.091	2.38	3.422	3.447	−0.026	0.74
H6a	3.913	3.823	0.090	2.34	3.966	3.879	0.088	2.26
H6b	3.768	3.745	0.023	0.62	3.753	3.704	0.049	1.32
MAD			0.110	2.98			0.073	2.07
R				0.9773				0.9763

(MAD = mean absolute deviation between the calculated and experimental values).

Table 5. Comparison of the calculated and the experimental (D_2O, 30 °C) δ_C values (ppm) of α-(**1a**) and β-D-glucopyranose (**1b**)

	α-D-Glucopyranose (**1a**)				β-D-Glucopyranose (**1b**)			
	Calcd	Exptl.	Δδ (ppm)	|Δδ| (%)	Calcd	Exptl.	Δδ (ppm)	|Δδ| (%)
C1	104.74	92.77	11.97	12.9	108.59	96.59	12.00	12.4
C2	82.14	72.15	9.97	13.8	85.01	74.81	10.20	13.6
C3	83.96	73.43	10.53	14.3	86.00	76.43	9.57	12.5
C4	79.55	70.32	9.23	13.1	79.23	70.27	8.96	12.8
C5	81.89	72.10	9.79	13.6	86.58	76.61	9.97	13.0
C6	70.10	61.27	8.83	14.4	70.18	61.42	8.76	14.3
MAD			10.06	13.7			9.91	13.1
R				0.9996				0.9997

(MAD = mean absolute deviation between the calculated and experimental values).

Table 6. Comparison of the calculated and the experimental (D_2O, 30 °C) $J_{H,H}$ values (Hz) of α-(**1a**) and β-D-glucopyranose (**1b**)

	α-D-Glucopyranose (**1a**)				β-D-Glucopyranose (**1b**)			
	Calcd	Exptl.	Δ*J* (Hz)	|Δ*J*| (%)	Calcd	Exptl.	Δ*J* (Hz)	|Δ*J*| (%)
$J_{H1,H2}$	4.59	3.80	0.79	20.8	7.75	7.97	−0.22	2.7
$J_{H1,H3}$	−0.45	−0.39	−0.06	14.7	0.00	n.r.	—	—
$J_{H1,H5}$	−0.80	−0.53	−0.27	51.1	−0.01	n.r.	—	—
$J_{H2,H3}$	9.83	9.84	−0.01	0.1	9.58	9.46	0.12	1.2
$J_{H3,H4}$	9.26	9.17	0.09	1.0	9.11	9.17	−0.06	0.7
$J_{H4,H5}$	10.06	9.99	0.07	0.7	9.74	9.92	−0.18	1.8
$J_{H5,H6a}$	4.00	2.31	1.69	73.1	3.84	2.27	1.57	69.0
$J_{H5,H6b}$	6.23	5.40	0.83	15.4	7.49	5.95	1.54	25.8
$J_{H6a,H6b}$	−13.01	−12.37	−0.64	5.2	−12.99	−12.30	−0.69	5.6
MAD			0.49	20.2			0.62	15.3
R				0.9959				0.9943

(n.r. = not resolved; MAD = mean absolute deviation between the calculated and experimental values).

from the experimental value, and the calculated $^{3}J_{H5,H6}$ values deviate between 0.9 and 1.7 Hz (15–73%) from the experimental ones (Table 6). On the other hand, the absolute deviations between the calculated and experimental values of the other couplings between the ring protons are small (0.01–0.27 Hz) (Table 6). The mean absolute deviation is 0.4 Hz and the percentual mean absolute deviation is 5.5% for all the couplings larger than 5 Hz. For small couplings (<5 Hz) the percentual deviations become easily large, and therefore, they were not included in the previous estimation. The established accuracy in the calculation of the NMR parameters is very good and indicates that the chosen level of theory performs very well. Overall, the largest differences are observed between the calculated and experimental $^{3}J_{H5,H6}$ values (Table 6) which indicate that the selected subsets of hydroxymethyl rotamers and their relative stabilities are, perhaps, not thoroughly modeling the complex equilibria of α- and β-D-glucose in aqueous solution. However, the calculated results support the correctness of the experimental results. Especially, the small long-range couplings observed for α-D-glucose are delightfully reproduced by the computations.

The calculated δ_H, δ_C, and $J_{H,H}$ values for the different rotamers (*gg*, *gt*, *tg*, gg_2, and gt_2) are presented in Tables S2–S7 in the Supplementary data.

2.7. Conclusions

All in all, the conformations of the sugar rings were not affected by the different glycosidic linkages or the anomeric protection. The ring $J_{H,H}$ values for the peracetylated glucopyranose (measured in $CDCl_3$) generally did not change more than 0.3 Hz in comparison to the corresponding values of glucose, the spectrum of which was recorded in water. The largest changes upon acetylation were detected in the $J_{H5,H6}$ values. The solvent and acetylation effects on the $J_{H,H}$ values were much smaller than we observed earlier for monosaccharides.[58] Small differences in the $J_{H4,H5}$ values of the disaccharides were observed in the reducing unit of the different anomers. In general $^{3}J_{H4,H5}$ for the α-anomer was >10 Hz while for the β-anomer it was observed to be <10 Hz, that is, approximately 0.2 Hz smaller than for the α-anomer (Table 2). The correlation between experimental and theoretically calculated NMR parameters (δ_H, δ_C, and $J_{H,H}$) was found to be good in general, and therefore, supports the correctness of the experimental results.

3. Experimental

All the disaccharides were commercially available (the highest available purity grades were purchased) and used as such without any further purification. '100%' D_2O was purchased from Euriso-top and $CDCl_3$ with 0.03% TMS from Aldrich.

3.1. NMR spectroscopy

All NMR spectra were recorded on a JEOL JNM A 500 or Bruker Avance spectrometer operating at 500.16 MHz for ^{1}H and 125.78 MHz for ^{13}C. 1D ^{1}H spectra were acquired with single-pulse excitation, 45° flip angle, pulse recycle time of 13 s, and with spectral widths of 5.5 kHz consisting of 64 k data points (digital resolution 0.08 Hz/pt), zero-filled to 256 k prior to Fourier transformation. The ^{13}C spectra were acquired with single-pulse excitation, 45° flip angle, pulse recycle time of 3.9 s, and with spectral widths of 34 kHz consisting of 64 k data points (digital resolution 0.53 Hz/pt), zero-filled to 128 k and with 0.5 Hz exponential weighting generally applied prior to FFT. The probe temperature was maintained at 303.15 K by a variable-temperature unit. All chemical shifts are quoted on the δ-scale in parts per million (ppm). The chemical shift scales are internally referred to the non-deuterated DMSO singlets at 2.71 ppm and 39.39 ppm in D_2O for ^{1}H and ^{13}C, respectively.[59] The anomeric carbons, as well as the protons, can be separated based on their homo- and heteronuclear coupling constants. Selective 1D TOCSY was also successfully utilized to distinguish between the different spin systems.

Normal 2D techniques were used like DQF-COSY, *J*-resolved spectroscopy, TOCSY (with spin-lock ranging from 20 to 250 ms), HSQC, HMBC ($^{1}J_{H,C}$ was set to 145 Hz and $^{n}J_{H,C}$ varying from 2 to 10 Hz), HSQC–TOCSY (with spin-lock ranging from 50 to 300 ms), and INADEQUATE, gradient enhanced versions were used where it was possible.

3.2. Computational methods

All the DFT geometry optimizations and nuclear spin–spin coupling calculations were performed with GAUSSIAN 03 program package utilizing the hybrid B3LYP exchange-correlation functional.[60] In the geometry optimizations the 6-31G(d,p) basis set was used. For the optimized structures, the nuclear shieldings (σ) and all the terms [Fermi contact (FC), spin-dipole (SD), para- and diamagnetic spin–orbit (PSO and DSO, respectively)] contributing to the *J*-couplings were calculated at the B3LYP/pcJ-2 level and the results were not scaled. The pcJ-2 basis set is specially designed for the calculation of nuclear spin–spin coupling constants.[61] The contraction scheme recommended by Jensen for the pcJ-2 basis set was used. For reference, the nuclear shieldings of tetramethylsilane (TMS) were calculated at the same level and the chemical shifts were then obtained by subtracting the isotropic shielding of each nucleus from the relevant reference shielding, $\delta_i =$

$\sigma_{ref} - \sigma_i$. Finally for α- and β-D-glucose, population weighted averages of the coupling constants were calculated. The populations of the various conformers were obtained from their relative stability differences in solution calculated utilizing the IEF-PCM method (see Supplementary data).[21]

The computational spectral analysis of the ^{1}H-spectra using PERCH NMR software was started from the spectral parameters extracted by the above outlined assignment procedure as described in the literature.[51] The refined spectral parameters were compared with the predicted ones and larger deviations were checked to ensure correct assignments.

Acknowledgments

Financial support from Danisco Sweeteners Oy, Glycoscience Graduate School, Research Foundation of Orion Corporation, and Stiftelsens för Åbo Akademi forskningsinstitut are gratefully acknowledged. The Finnish IT center for science (CSC) is acknowledged for the allocated computing time.

Supplementary data

Supplementary data associated with this article can be found, in the online version, at doi:10.1016/j.carres.2007.10.008.

References

1. Jiménez-Barbero, J.; Peters, T. *NMR Spectroscopy of Glycoconjugates*; Wiley-VCH: Weinheim, 2003.
2. Duus, J. Ø.; Gotfredsen, C. H.; Bock, K. *Chem. Rev.* **2000**, *100*, 4589–4614.
3. Morris, G. A.; Hall, L. D. *Can. J. Chem.* **1982**, *60*, 2431–2441.
4. Hoffman, R. E.; Christofides, J. C.; Davies, D. B.; Lawson, C. J. *Carbohydr. Res.* **1986**, *153*, 1–16.
5. Morris, G. A.; Hall, L. D. *J. Am. Chem. Soc.* **1981**, *103*, 4703–4711.
6. Laurance, H. D.; Morris, G. A.; Sukumar, S. *J. Am. Chem. Soc.* **1980**, *102*, 1745–1747.
7. Christofides, J. C.; Davies, D. B. *J. Am. Chem. Soc.* **1983**, *105*, 5099–5105.
8. Bock, K.; Thøgersen, H. *Ann. Rep. NMR Spectrosc.* **1982**, *13*, 1–57.
9. Kalinowski, H.-O.; Berger, S.; Braun, S. *Carbon-13 NMR Spectroscopy*; John Wiley & Sons: Chippenham, 1988.
10. Jansson, P.-E.; Kenne, L.; Schweda, E. *J. Chem. Soc., Perkin Trans. 1* **1988**, 2729–2736.
11. Forsgren, M.; Jansson, P.-E.; Kenne, L. *J. Chem. Soc., Perkin Trans. 1* **1985**, 2383–2388.
12. Backman, I.; Erbing, B.; Jansson, P.-E.; Kenne, L. *J. Chem. Soc., Perkin Trans. 1* **1998**, 889–898.
13. De Bruyn, A.; Antenius, M.; Verhegge, G. *Bull. Soc. Chim. Belg.* **1975**, *84*, 721–734.
14. Angyal, S. J. *Adv. Carbohydr. Chem. Biochem.* **1984**, *42*, 15–68.
15. Zhu, Y.; Zajicek, J.; Serianni, A. S. *J. Org. Chem.* **2001**, *66*, 6244–6251.
16. Maddox, J. *Nature* **1993**, *364*, 669.
17. Barrows, S. E.; Dulles, F. J.; Cramer, C. J.; French, A. D.; Truhlar, D. G. *Carbohydr. Res.* **1995**, *276*, 219–251.
18. Csonka, G.; Éliás, K.; Csizmadia, I. G. *Chem. Phys. Lett.* **1996**, *257*, 49–60.
19. Appell, M.; Strati, G.; Willett, J. L.; Momany, F. A. *Carbohydr. Res.* **2004**, *339*, 537–551.
20. Corchado, J. C.; Sánchez, M. L.; Aguilar, M. A. *J. Am. Chem. Soc.* **2004**, *126*, 7311–7319.
21. da Silva, C. O.; Mennucci, B.; Vreven, T. *J. Org. Chem.* **2004**, *69*, 8161–8164.
22. Momany, F. A.; Appell, M.; Willett, J. L.; Bosma, W. B. *Carbohydr. Res.* **2005**, *340*, 1638–1655.
23. Nishida, Y.; Hori, H.; Ohrui, H.; Meguro, H. *J. Carbohydr. Chem.* **1988**, *7*, 239–250.
24. Nishida, Y.; Ohrui, H.; Meguro, H. *Tetrahedron Lett.* **1984**, *25*, 1575–1578.
25. Polavarapu, P. L.; Ewig, C. S. *J. Comput. Chem.* **1992**, *13*, 1255–1261.
26. Ma, B.; Schafer, H. F., III; Allinger, N. L. *J. Am. Chem. Soc.* **1998**, *120*, 3411–3422.
27. Lii, J.-H.; Ma, B.; Allinger, N. L. *J. Comput. Chem.* **1999**, *20*, 1593–1603.
28. Barrows, S. E.; Storer, J. W.; Cramer, C. J.; French, A. D.; Truhlar, D. G. *J. Comput. Chem.* **1998**, *19*, 1111–1129.
29. Kräutler, V.; Müller, M.; Hünenberger, P. H. *Carbohydr. Res.* **2007**, *342*, 2097–2124.
30. Poppe, L.; van Halbeek, H. *J. Am. Chem. Soc.* **1992**, *114*, 1072–1074.
31. Adams, B.; Lerner, L. *J. Am. Chem. Soc.* **1992**, *114*, 4827–4829.
32. Molteni, C.; Parrinello, M. *J. Am. Chem. Soc.* **1998**, *120*, 2168–2171.
33. Cramer, C. J.; Truhlar, D. G. *J. Am. Chem. Soc.* **1993**, *115*, 5745–5753.
34. Klein, R. A. *J. Am. Chem. Soc.* **2002**, *124*, 13931–13937.
35. Klein, R. A. *J. Comput. Chem.* **2003**, *24*, 1120–1131.
36. Cloran, F.; Carmichael, I.; Serianni, A. S. *J. Am. Chem. Soc.* **1999**, *121*, 9843–9851.
37. Stortz, C. A.; Cerezo, A. S. *J. Carbohydr. Chem.* **2003**, *22*, 217–239.
38. Koney, D.; Damm, W.; Stoll, S.; Hünenberger, P. H. *J. Phys. Chem. B* **2004**, *108*, 5815–5826.
39. Rao, V. S. R.; Qasba, P. K.; Balaji, P. V.; Chandrasekaren, R. *Conformation of Carbohydrates*; Harwood Academic: Amsterdam, 1998.
40. Ivarsson, I.; Sandström, C.; Sandström, A.; Kenne, L. *J. Chem. Soc., Perkin Trans. 2* **2000**, 2147–2152.
41. Bekiroglu, S.; Kenne, L.; Sandström, C. *J. Org. Chem.* **2003**, *68*, 1671–1678.
42. Eijck, B. P.; Mooij, W. T. M.; Kroon, J. *J. Phys. Chem. B* **2001**, *105*, 10573–10578.
43. Zhao, H.; Pan, Q.; Zhang, W.; Carmichael, I.; Serianni, A. S. *J. Org. Chem.* **2007**, *72*, 7071–7082.
44. Pan, Q.; Klepach, T.; Carmichael, I.; Reed, M.; Serianni, A. S. *J. Org. Chem.* **2005**, *70*, 7542–7549.
45. Stenutz, R.; Carmichael, I.; Widmalm, G.; Serianni, A. S. *J. Org. Chem.* **2002**, *67*, 949–958.
46. Roën, A.; Padrón, J. I.; Vázquez, J. T. *J. Org. Chem.* **2002**, *68*, 4615–4630.
47. French, A. D.; Johnson, G. P.; Kelterer, A.-M.; Csonka, G. I. *Tetrahedron: Asymmetry* **2005**, *16*, 577–586.

48. Bell, A. F.; Hecht, L.; Barron, L. D. *J. Am. Chem. Soc.* **1994**, *116*, 5155–5161.
49. Bell, A. F.; Hecht, L.; Barron, L. D. *J. Raman Spectrosc.* **1995**, *26*, 1071–1074.
50. Taniguchi, T.; Monde, K. *Org. Biomol. Chem.* **2007**, *5*, 1104–1110.
51. Laatikainen, R.; Niemitz, M.; Weber, U.; Sundelin, J.; Hassinen, T.; Vepsäläinen, J. *J. Magn. Reson., Ser. A* **1996**, *120*, 1–10.
52. Tvaroska, I.; Taravel, F. R. *Adv. Carbohydr. Chem. Biochem.* **1995**, *51*, 15–62.
53. Breitmaier, E. *Structure Elucidation by NMR in Organic Chemistry*, 3rd ed.; John Wiley & Sons: Chichester, 2002, p 46.
54. Laatikainen, R.; Niemitz, M.; Malaisse, W. J.; Biesemans, M.; Willem, R. *Magn. Reson. Med.* **1996**, *36*, 359–365.
55. PERCH NMR software v.2007.1, PERCH Solutions Ltd, Kuopio, Finland. www.perchsolutions.com.
56. Bagno, A.; Saielli, G. *Theor. Chem. Acc.* **2007**, *117*, 603–619.
57. *Calculation of NMR and EPR Parameters*; Kaupp, M., Bühl, M., Malkin, V. G., Eds.; Wiley-VCH: Weinheim, 2004.
58. Roslund, M. U.; Klika, K. D.; Lehtilä, R. L.; Tähtinen, P.; Sillanpää, R.; Leino, R. *J. Org. Chem.* **2004**, *69*, 18–25.
59. Gottlieb, H. E.; Kotlyar, V.; Nudelman, A. *J. Org. Chem.* **1997**, *62*, 7512–7515.
60. Frisch, M. J.; Trucks, G. W.; Schlegel, H. B.; Scuseria, G. E.; Robb, M. A.; Cheeseman, J. R.; Montgomery Jr., J. A.; Vreven, T.; Kudin, K. N.; Burant, J. C.; Millam, J. M.; Iyengar, S. S.; Tomasi, J.; Barone, V.; Mennucci, B.; Cossi, M.; Scalmani, G.; Rega, N.; Petersson, G. A.; Nakatsuji, H.; Hada, M.; Ehara, M.; Toyota, K.; Fukuda, R.; Hasegawa, J.; Ishida, M.; Nakajima, T.; Honda, Y.; Kitao, O.; Nakai, H.; Klene, M.; Li, X.; Knox, J. E.; Hratchian, H. P.; Cross, J. B.; Bakken, V.; Adamo, C.; Jaramillo, J.; Gomperts, R.; Stratmann, R. E.; Yazyev, O.; Austin, A. J.; Cammi, R.; Pomelli, C.; Ochterski, J. W.; Ayala, P. Y.; Morokuma, K.; Voth, G. A.; Salvador, P.; Dannenberg, J. J.; Zakrzewski, V. G.; Dapprich, S.; Daniels, A. D.; Strain, M. C.; Farkas, O.; Malick, D. K.; Rabuck, A. D.; Raghavachari, K.; Foresman, J. B.; Ortiz, J. V.; Cui, Q.; Baboul, A. G.; Clifford, S.; Cioslowski, J.; Stefanov, B. B.; Liu, G.; Liashenko, A.; Piskorz, P.; Komaromi, I.; Martin, R. L.; Fox, D. J.; Keith, T.; Al-Laham, M. A.; Peng, C. Y.; Nanayakkara, A.; Challacombe, M.; Gill, P. M. W.; Johnson, B.; Chen, W.; Wong, M. W.; Gonzalez, C.; Pople, J. A. GAUSSIAN *03, Revision C.02*; Gaussian: Wallingford, CT, 2004.
61. Jensen, F. *J. Chem. Theor. Comput.* **2006**, *2*, 1360–1369.